

# Erosion shock wave in laminar flumes

O. Devauchelle, L. Malverti, É. Lajeunesse & F. Métivier  
*Institut de Physique du Globe de Paris, France*

P.-Y. Lagrée, C. Josserand & S. Zaleski  
*Institut Jean Le Rond d'Alembert, Université Pierre & Marie Curie, Paris, France*

**ABSTRACT:** The present paper investigates the formation of the rhomboid pattern appearing when a granular layer is eroded by a laminar flow. As in turbulent rivers, laminar flows can generate unstable erosion waves. These instabilities, which provide the classical explanation for alternate bars formation, propagate in a direction inclined with respect to the main flow. Through numerical simulations, we demonstrate that this instability becomes an erosion shock wave, which in turn results in diamond-shaped patterns. An experimental set-up able to reproduce this instability is also briefly presented.

## 1 INTRODUCTION

When walking on the foreshore one may notice the presence of a small (a few centimeters), fine and regular rhomboid pattern, as the one presented on Figure 1. Similar patterns were experimentally obtained by Daerr et al. (2003), when withdrawing a plate covered with a granular material from a bath of water, at constant angle and velocity.

The striking regularity of the pattern may lead to incriminate a purely hydrodynamic instability (the crossing stationary gravity waves in super-critical flumes often result in comparable patterns). The sand topography deformation would then only be the mark of an inhomogeneous water velocity field. The experiments of Daerr et al. (2003) suggest that a transverse instability of the moving contact line at the intersection of water and sediments surfaces might be responsible for the appearance of this erosion patterns. However, most experimental runs lie outside the existence domain of a contact line (see Devauchelle et al. 2007a). This invalidates the contact-line instability hypothesis.

The present paper aims to demonstrate that the bank instability, well-known in rivers since the work of Callander (1969), is a good candidate to represent the initial steps of rhomboid patterns development. It is not exceptional in Geomorphology that a large-scale phenomenon, naturally occurring in turbulent rivers, has a laminar counterpart. Even if direct up-scaling should not be expected in general, it has been recently demonstrated that the mechanisms of erosion by water flows in laminar and turbulent regimes are very comparable. This statement holds in various

situations, from alternate bars to gravity currents, including meanders and braids (Malverti et al. 2007; Malverti et al. 2008; Métivier et al. 2005; Smith 1998; Devauchelle et al. 2007b). Such analogy justifies the use of small-scale experimental set-up to better understand the fundamental features of erosion pattern formation.

In the present article, a simple two-dimensional model is proposed to represent erosion by laminar flow. It is then analyzed to show how the non-linearity of a classical sediment transport law may generate a propagating erosion front. Numerical analysis demonstrate that the crossing of symmetric fronts leads to the formation of rhomboid patterns. Finally, we briefly present preliminary experimental experiments designed to reproduce the formation of these patterns under controlled conditions.



Figure 1. Erosion rhomboid pattern appearing on a beach near Goleta, California, USA. The mean width of a single rhombus is approximately 5 cm.

## 2 TWO-DIMENSIONAL MODEL

### 2.1 Equations

The model presented in this section has been simplified as much as possible, while keeping the essential features of bank instability. It is directly inspired by those commonly used in river Geomorphology, and adapted to laminar flows. It can certainly be improved on many points (sediment transport law, slip condition for the bottom water velocity), but our purpose here is only to demonstrate its ability to represent the formation of rhomboid patterns.

The full problem consists in solving the Saint-Venant (shallow water) equations coupled with the following equation of mass conservation for sediments (Exner Equation):

$$\frac{\partial h}{\partial t} = -\nabla \cdot \mathbf{q}, \quad (1)$$

where the starred quantities are non dimensional and  $\mathbf{q}_*$  is the flux of mass sediments. It is linked to the horizontal projection of the skin friction :

$$\mathbf{q}_* = \|\tau_*\|^\beta \left( \frac{\mathbf{u}_*}{\|\mathbf{u}_*\|} - \gamma \mathcal{N} h_* \right), \quad (2)$$

Where gamma determines the slope effect coefficient. The exponent beta reflects the non-linearity of the transport law (Shielen et al. 1993).

The Saint-Venant equations may be linearized for a small perturbation of the topography as:

$$\frac{6F^2}{5} \frac{\partial u}{\partial x} = -\frac{\partial \eta}{\partial x} - S(2h + u - 2\eta) \quad (3)$$

$$\frac{6F^2}{5} \frac{\partial v}{\partial x} = -\frac{\partial \eta}{\partial y} - S v \quad (4)$$

$$\frac{6F^2}{5} \frac{\partial v}{\partial x} = -\frac{\partial \eta}{\partial y} - S v \quad (5)$$

where  $(u, v)$  are the averaged linearized water velocities over the water depth, respectively in the  $(x, y)$  direction. The mean slope of the topography  $h$  in the longitudinal direction  $x$  is denoted by  $S$ .  $F$  is the Froude number. The surface elevation is  $h$ . The linearized skin friction reads

$$\tau_x = u - \eta + h \quad (6)$$

Nevertheless we do not linearize the sediment equation since it is the main nonlinear effect (Hall 2006). We only linearize its directional part.

$$q_x = (1 + \tau_x)^\beta (1 - \gamma \partial_x h), q_y = (1 + \tau_x)^\beta (v - \gamma \partial_y h) \quad (7)$$

## 3 LINEAR STABILITY

The above system of equations admits a trivial uniform solution on the horizontal plane:  $h$ ,  $u$  and  $q_x$  are equal to one, while any transverse flux vanishes. Sediment transport indeed occurs, but does not lead to any deformation of the topography as a consequence of its uniformity.

In many cases, this state is linearly unstable. If it is perturbed with an erosion wave of the form

$$h = e^{i(\mathbf{k} \cdot \mathbf{x} - \omega t)} \quad (6)$$

where  $\mathbf{k}$  is the perturbation wavenumber, and  $\omega$  its complex pulsation. The stability of the erosion wave depends on the sign of the imaginary part of the pulsation,  $\Im(\omega)$ . Figure 2 presents this imaginary part plotted under typical flow conditions.

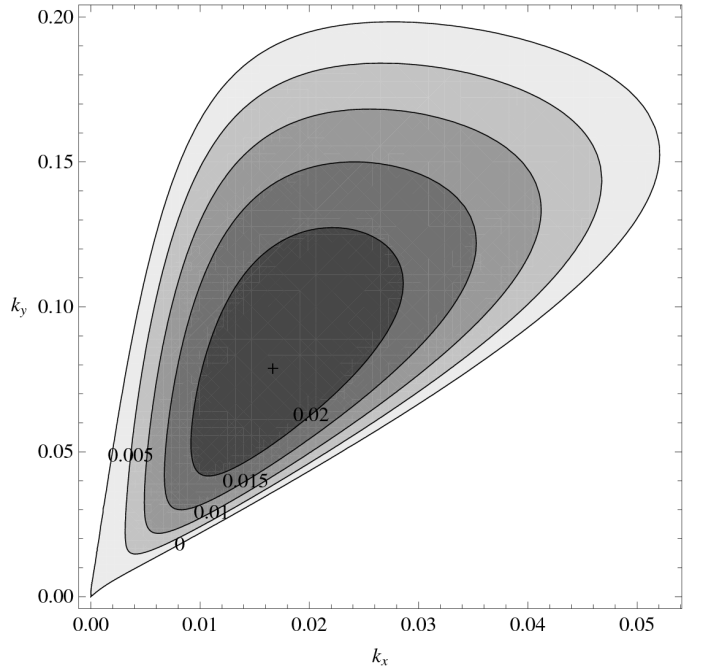


Figure 2. Bank instability growth rate  $\Im(\omega)$  as a function of the wave vector  $\mathbf{k}$ .

The most instable waves are inclined with respect to the main flow direction (the figure is symmetrical with respect to the  $x$ -axis), whereas no instability can develop in the flow direction. This property results from the inability of Saint-Venant equation to reproduce ripple formation. In rivers, where bank conditions must be imposed, the sum of two symmetrical erosion waves leads to alternate bars formation (see Callander 1969).

The bank instability presented on Figure 2 is not based on inertia. Indeed, if the Froude number  $F$  is set to zero in equations (3) and (4), an instable erosion wave with similar characteristics can still develop. This results holds for both laminar and turbulent flows.

## 4 NON-LINEAR EVOLUTION

The fully non-linear versions of equations (1) to (5) can be numerically solved. It is thus possible to follow the growth of an erosion wave of finite amplitude. As presented on Figure 3, non-linearities affect the shape of a single sinusoidal wave.

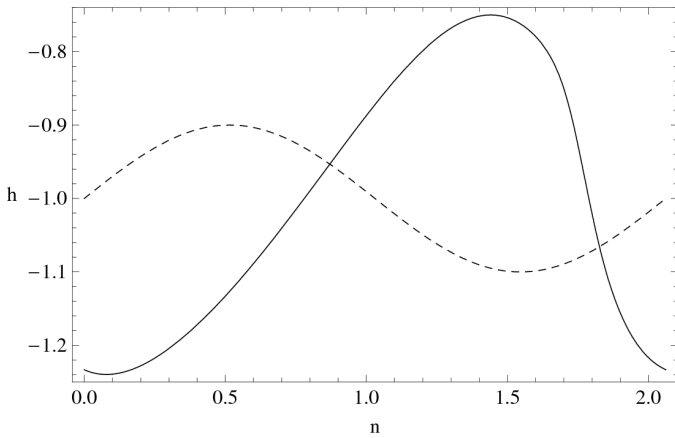


Figure 3. Evolution of an isolated erosion wave (numerical simulation). Non linear terms in the erosion equations lead to a steep front formation.  $n$  denotes the propagation direction.

The downstream sides of the perturbation steepen, until an abrupt front is formed. This mechanism is reminiscent of shock wave formation in gases.

As the steepness of the front increases, the sediment diffusion mechanism due to gravity, represented in Equation (2) by the term proportional to  $\gamma$ , slows down the wave growth. Eventually, an equilibrium shape of amplitude  $h_{max}$  is reached, which propagates without being deformed.

As long as the wave amplitude remains small enough, the flow equations may be linearized. The main non-linear effect is then due to the erosion law (2), where  $\beta$  plays the role of a tuning coefficient controlling the non-linearity of the sediment transport relation. This idea was successfully introduced by Hall (2006) for turbulent rivers.

We used the same approximation to numerically determine the saturation amplitude of erosion shock waves, for different values of the  $\beta$  parameter. These results are plotted on Figure 4. Below a certain critical value  $\omega_c$ , which depends on the other parameters values, an erosion wave remains stable. Above this value, the saturation amplitude  $h_{max}$  grows nearly as a square root function of  $\beta$ , indicating a super-critical bifurcation.

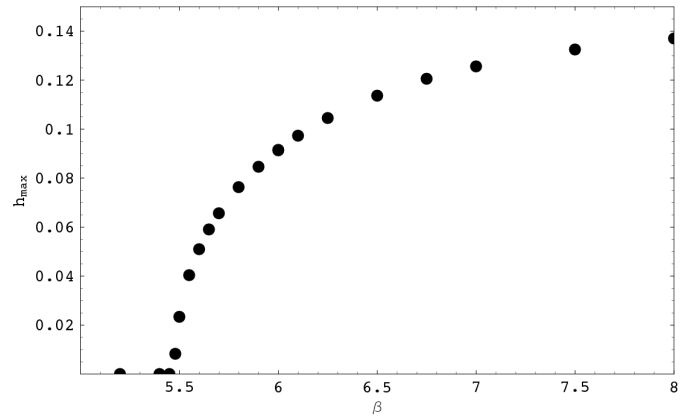


Figure 4. Saturation amplitude  $h_{max}$  of the erosion wave vs. the erosion law parameter  $\beta$ .

Here, it should be noted that even though we simplified the analysis through the use of a power erosion law, the same results could be obtained with a different law, provided the skin friction remains at a finite distance from any threshold.

## 5 FORMATION OF A DIAMOND-SHAPED PATTERN

### 5.1 Numerical simulations

Under natural or experimental conditions, one cannot observe the development of a single sinusoidal mode. Instead, the boundary conditions, as well as the initially perturbed bed topography leads to the co-existence of the two symmetrical modes. The crossing of the two shock waves issued from these modes forms a typical diamond-shaped pattern.

This result can be reproduced numerically, as shown on Figure 5. The opening angle of the fully developed rhombi (about  $25^\circ$ ) is close to the angle between the two most instable linear modes. This similarity is an indication that the bank instability is responsible for the formation of rhomboid erosion patterns.

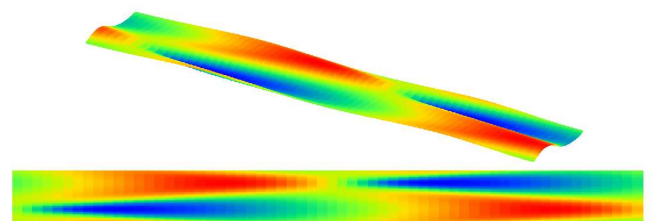


Figure 5. Numerical simulation of crossed erosion fronts under laminar flows conditions. Hall (2006) presented similar results in turbulent rivers.

Hall (2006) first proposed a similar mechanism in rivers, for turbulent flows at a much larger scale. The existence of large banks inclined with respect to the main flow direction was also pointed out in marine conditions by Idier & Astruc (2003).

We were able to reproduce experimentally rhomboid patterns by eroding a bed of silica powder by a laminar flow (the Reynolds number being of the order of 100). An example from these experiments is presented on Figure 6. As the experimental parameters are varied, the size of a rhombus (that is, the mode of the instability) varies. This variations reflects the transition between the most instable modes of the bank instability (see Devauchelle et al. 2007).

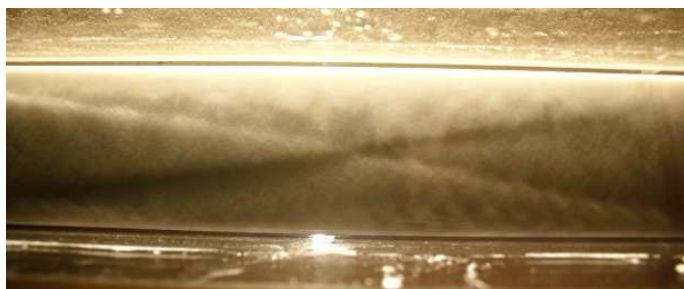


Figure 6. Diamond-shaped erosion pattern formed in a laminar experimental flume. The bed is made of silica beads which mean diameter is 100  $\mu\text{m}$ . The width of the channel is 5 cm, and the flow height about 5 mm.

The experimental erosion shock wave quickly reach an invariant shape, and propagates downstream. Their velocities are about 1-10  $\text{mm}\cdot\text{s}^{-1}$ .

## 6 CONCLUSIONS

This study proposes a simple two-dimensional model able to reproduce, at least qualitatively, the diamond-shaped erosion patterns first pointed out by Daerr et al. (2003). The instability involved in their formation is that of alternate bars, which is based on the interaction between flow and sediment transport. This coupled mechanism cannot be reduced to a purely hydrodynamic feature, as it is often the case in Geomorphology, see the meandering theories of Ikeda et al. (1981) and Blondeau & Seminara (1985).

Besides the practical interest of investigating the formation and displacement of sandbanks, the study of erosion rhomboid patterns might provide new tools to the query of sediment transport laws. Indeed, the main characteristics of these patterns, namely their opening angle and velocity, can easily be measured. If the dependence of these characteristics with respect to the erosion law are theoretically understood, they can provide additional information to experimentalists. As long as the amplitude of the erosion shock waves remains small enough, they will not perturb the global sediment flux of the basic

state, which may be measured simultaneously and independently.

## 7 REFERENCES

- Blondeaux, P. & Seminara G. 1985. A unified bar-bend theory of river meanders. *J. Fluid Mech.* 157: 449–470.
- Callander, R.A. 1969. Instability and river channels. *J. Fluid Mech.* 36(3): 465–480.
- Daerr, A., Lee, P., Lanuza, J. & Clément, É. 2003. Erosion patterns in a sediment layer. *Phys. Rev. E* 67: 065201.
- Devauchelle, O., Josserand, C. & Zaleski, S. 2007a. Forced dewetting on porous media. *J. Fluid Mech.* 574: 343–364.
- Devauchelle, O., Josserand, C., Lagrée, P.-Y. & Zaleski, S. 2007b. Morphodynamic modeling of erodible laminar channels. *Phys. Rev. E* 76: 056318.
- Hall, P. 2006. Nonlinear evolution equations and the braiding of weakly transporting flows over gravel beds. *Studies in Applied Mathematics* 117: 27–69.
- Idier, D. & Astruc, D. 2003. Analytical and numerical modeling of sandbanks dynamics. *Journal of Geophysical Research* 108 (C3): 3060.
- Ikeda, S., Parker, G. & Saway, K. 1981. Bend theory of river meanders. Part 1. Linear development. *J. Fluid Mech.* 112:363–377.
- Malverti, L., Lajeunesse, É. & Métivier, F. 2007. Experimental investigation of the response of an alluvial river to a vertical offset of its bed. In Dohmen-Janssen & Hulscher (eds) *River, Coastal and Estuarine Morphodynamics*, Taylor & Francis Group: London.
- Malverti, L., Lajeunesse, É. & Métivier, F. 2008. Small is beautiful: upscaling from microscale laminar to natural turbulent rivers. *Submitted to Journal of Geophysical Research*.
- Métivier, F., Lajeunesse, É. & Cacas, M.-C. 2005. Submarine canyons in the bathtub. *Journal of sedimentary research* 75(1): 6–11.
- Smith, C.E. 1998. Modeling high sinuosity meanders in a small flume. *Geomorphology* 25: 19–30.